Progress In Electromagnetics Research C, Vol. 68, 129–139, 2016

Randomly Overlapped Subarrays for Angular-Limited Scan Arrays

Davide Bianchi[1, 2], Simone Genovesi[1, 2, *], and Agostino Monorchio[1, 2]

Abstract—This work investigates the performance improvements in terms of sidelobe reduction provided by arrays organized into randomly overlapped subarrays (ROSAs) in comparison to other subarray arrangements such as contiguous and uniformly-overlapped modules. This configuration can be advantageous for applications that need to scan over a limited angular sector. The performance of the ROSA design is thoroughly analyzed for different degrees of overlapping in terms of scan losses, minimization of peak side lobe level, number of components and array size.

1. INTRODUCTION

It is well known that large phased arrays are generally organized into subarrays for reasons of scalability, mechanical constraints and limitation of the number of steering units required for beam scanning and the effort in proposing novel solutions is uninterrupted [1–4]. Among the many requirements for different applications, a challenging task is represented by arrays that exhibit a high-directivity beam and low peak side lobe level while scanning an angular-limited sector. This may be the case of the limited field of view (LFOV) arrays, which are large arrays employed in synchronous satellites systems for scanning the beam over angles of few degrees to perform detailed mapping of the ground surface or for small areas coverage. In case of wideband arrays scanning over a limited angular sector, equipping each element with a time delay control is considered an unfeasible option because of the difficulty of implementing TDs at the element level or switched TD line. Digital or optical beamforming networks can successfully introduce a time delay at element or subarray level even though this solution has a significant impact on the system cost. Therefore, it is often convenient to introduce time delay at the subarray level in order to employ a relatively small number of time delay units. For the aforementioned reasons, we are considering arrays that do not possess TD units at element level but the delay lines are supposed to be connected at the input port of each subarray in order to perform the beam scanning. The simplest way of organizing the array into subarrays is to group the radiating elements into identical contiguous subarrays that are uniformly distributed across the radiating aperture. Unfortunately, this periodic arrangement is affected by quantization lobes that occur at the grating lobe locations of the array created by the subarray phase centers. In fact, the quantization lobes arise because the subarray pattern radiates broadside and it is stationary, whereas the array factor is scanned. Although a guideline for selecting the subarray spacing exists to suppress the quantization lobes during the main beam scanning, this criterion represents a theoretical upper bound limit because it is achieved only by using an idealized pulse-shaped subarray pattern. Among the techniques proposed to reach this upper bound limit, one of the best solution is represented by the so-called dual transform or overlapped subarray network. This configuration employs a multiple-beam feed and a focusing lens to form a periodically-spaced and completely-overlapped set of beams illuminating an aperture for radiating an approximately pulse-shaped subarray pattern [5]. Although this solution provides high performances, such a system is not compact since the overall feed

Received 6 June 2016, Accepted 3 September 2016, Scheduled 14 October 2016

* Corresponding author: Simone Genovesi (simone.genovesi@iet.unipi.it).

[1] Department of Information Engineering, University of Pisa, Via G. Caruso, Pisa 56122, Italy. [2] RaSS — Consorzio Nazionale Interuniveristario per le Telecomunicazioni (CNIT), Galleria Gerace 18, 56100 Pisa, Italy.

network may result in a bulky structure and because an amplitude tapering is required at subarray level at least to achieve low peak side lobe level (pSLL). Other recent works on overlapped subarrays prove the actual interest in overlapped subarray architectures and their feasibility in real-world applications [6, 7]. A viable strategy to overcome the quantization lobe problem relies on exploiting aperiodicity and randomness in the radiating element arrangement or excitations [8–10]. This method may produce a sparse array covering electrically-large areas thus avoiding the occurrence of the quantization lobes determined by a periodic element lattice.

The solution investigated in this work to obtain a low pSLL and, at the same time, reducing the steering units consists in altering the periodicity by randomly placing subarrays with suitable dimensions with a proper factor of aperiodic overlap. The benefits of exploiting randomly-overlapped subarray configurations in comparison with non-overlapped and periodic overlapped schemes will be investigated in detail. In particular, the unique features of an overlapped subarray configuration will be compared to those of a regular overlapped arrangement under the widely adopted hypothesis [11–13] of neglecting the mutual coupling between the radiating elements. Although the proposed array configuration can be useful even in the case of wideband scanning array [14], the results presented in this paper are focused only at angular-limited scan array case. The performance of a randomly overlapped arrangement of subarrays will be analyzed for different overlapping factors in terms of scan losses, minimization of peak side lobe level, beamforming network and array dimension.

2. OVERLAPPED SUBARRAY LAYOUTS

Overlapped subarrays share one or more of the edge elements of the adjacent subarray, hence each array element may be coupled to more than one source port. A linear array is considered in order to show the effectiveness of randomly overlapping the subarrays in order to achieve a better sidelobe level with respect to place them contiguously or periodically overlapped. As an example, an array comprising 50 isotropic elements, which are half-wavelength-spaced apart at the highest frequency, is arranged into 5-element subarrays. Three different array layouts are analyzed and their performance are evaluated and compared. More in detail, the first array is composed by 10 contiguous subarrays (Fig. 1(a)). As a constraint, we consider that all the subarrays are equal and each one is connected to a single source port with a dedicated steering unit so that all the elements of a subarray are in phase. The second one comprises 16 uniformly-overlapped subarrays (Fig. 1(c)), whereas the last one has 16 randomly overlapped subarrays (Fig. 1(e)). All the considered arrays are symmetric with respect to the broadside axis.

The effect of overlapping some subarrays is investigated by observing, for each array layout, the subarray pattern (SP), array factor (AF) and overall radiation pattern (RP). They are reported and superimposed in Fig. 1 for the three aforementioned arrays, when the main beam is scanned broadside at the upper frequency. The subarrays are identical, therefore each subarray has the radiation pattern of 5 uniformly-spaced isotropic sources for all the three analyzed cases. On the other hand, the AF depends on the locations of the subarray sources and it differs from case to case. More in detail, the distance between the centers of two adjacent subarrays is 2.5λ for the case of contiguous subarrays (Figs. 1(a), (b)) and 1.5λ for the case of uniformly-overlapped subarrays (Figs. 1(c), (d)). As the subarray lattice is periodic (Fig. 1(a) and Fig. 1(c)) the array factor exhibits grating lobes that determines an increase in the overall peak sidelobe level. Furthermore, although the grating lobes can occur at a deep null location of the SP (Fig. 1(b)), the overall peak side lobe level around -13 dB is determined by the sidelobe of the array factor, as predicted by the theory. On the other hand, if the subarrays are randomly-overlapped, the AF does not show any grating lobes as a result of the introduced randomness of the subarray arrangement (Fig. 1(f)). In addition, in this case the AF sidelobes close to the main beam are lower than those of Fig. 1(b) and Fig. 1(d), thus determining a decrease of the peak side lobe level up to 20 dB below the main beam.

Finally, as the array is scanned up to 8° off broadside, the randomly overlapped subarray array still outperforms both the contiguous and the uniformly-overlapped subarray array in terms of sidelobe level reduction. As evident from Table 1, it is worth noting that lowering the peak sidelobe level is paid in terms of gain and HPBW decrease. For instance, in the randomly-overlapped subarray case, the gain reduces approximately by 0.7 dB on average with respect to that of the contiguous subarray layout

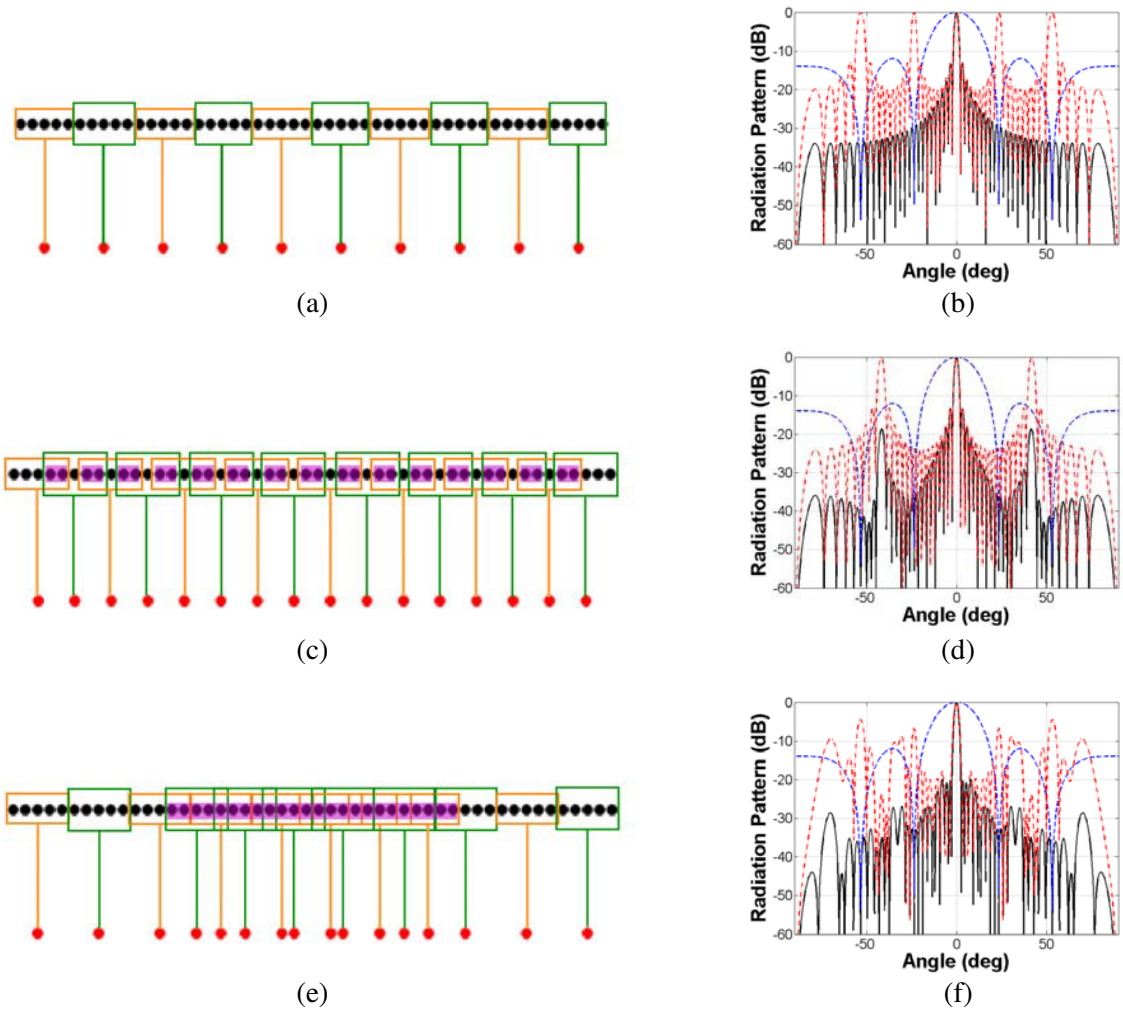

Figure 1. Array layouts and radiation patterns for: (a), (b) contiguous subarray; (c), (d) uniformly-overlapped subarrays; (e), (f) randomly-overlapped subarrays. Antenna elements are indicated by the black dots whereas the source port of each subarray is in red. Overlapped elements are highlighted in purple. The blue dashed line represents the subarray pattern (SP), the red dashed one the array factor (AF) and the continuous black one is the array pattern (RP).

Table 1. Radiation performance of the three arrays in Fig. 1.

	Scan angle = 0°		**Scan angle = 8°**	
	Gain (dB)	**HPBW (°)**	**Gain (dB)**	**HPBW (°)**
Contiguous subarray	16.99	2	15.27	2.1
Uniformly-overlapped subarray	16.6	2	14.88	2.1
Randomly-overlapped subarray	16.24	2.4	14.54	2.5

within the angular coverage. From the previous analysis, it can be inferred that the employment of a randomly overlapped subarray layout can provide a significant improvement in terms of peak sidelobe level reduction and this feature can be advantageously exploited in the design of angular-limited scan array.

3. DESIGN OF ANGULAR-LIMITED SCAN ARRAY BY USING RANDOMLY OVERLAPPED SUBARRAYS

In order to prove the effectiveness of the ROSA architecture in designing array with low peak sidelobe level and a reduced number of TD units, a linear array comprising a total number of elements equal to 201 ($NElemTot = 201$) placed at half-wavelength distance was optimized. The aim is to scan the main beam up to 10 degrees off broadside while keeping the sidelobe level at least below -20 dB in the scanning range. The constraint in the design is represented by considering equal subarrays as building blocks in order to simplify the array realization. After an exhaustive search based on all the allowed subarray dimensions, a subarray comprising 5 isotropic radiating elements ($NElemSub = 5$) has been selected for the design of the final ROSA array, which consists of 65 subarrays ($NSub = 65$). The arrangement of the elements is illustrated in Fig. 2(a), where the black and red lines represent the location of the elements and the subarray input ports, respectively.

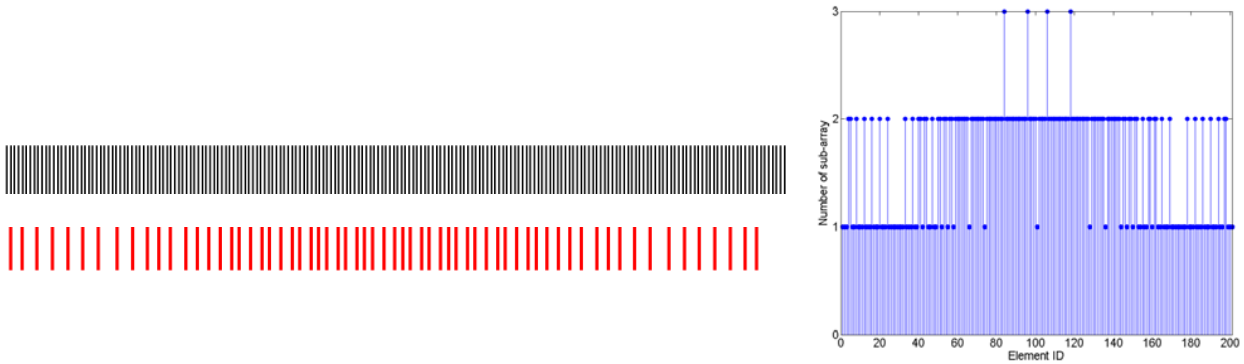

(a) (b)

Figure 2. (a) Array layout with the location of each element (black line) and the place of the subarray sources (red lines); (b) degree of overlapping for each one of the 201 elements. Number of subarrays which elements belong to is reported along y-axis.

From Fig. 2(a) it is worth noting that being the elements uniformly spaced half a wavelength at the maximum operating frequency, the element lattice is clearly regular and periodic whereas the subarray sources are randomly located, even though symmetric with respect to the broadside direction. The level of overlapping is illustrated in Fig. 2(b) where, for each one of the 201 elements, it is reported the number of subarrays that share that element. It is apparent that even if each subarray is uniformly excited, the signals combine at each overlapped element, resulting in a not uniform amplitude tapering at element level. More in detail, there are 116 elements that belong to two different subarrays and 4 that are connected to three subarrays with an overall degree of overlapping factor (OF) defined as:

$$OF = \frac{NSub \times NElemSub}{NElemTot} - 1 \tag{1}$$

which is over 60%. The change in the sidelobe level as the main beam is scanned off broadside over a 10 : 1 bandwidth is reported in Fig. 3.

It is also interesting to point out that the half-wavelength element periodicity at the highest frequency of a considered bandwidth determines closely-spaced elements at lower frequencies which improves the array bandwidth impedance matching, as in the case of connected dipoles or Vivaldi arrays [15]. Since both arrays, as well as the subarray lattices, are symmetric with respect to the broadside axis, for the sake of avoiding redundancy only the results for the positive scanning angles [0°–10°] are plotted. It is apparent that the -20 dB requirement on the peak sidelobe level is completely fulfilled within both the operating bandwidth and the scan angle range. It is interesting to notice that this goal has been achieved by employing only 65 TD units at the subarray input ports instead of a solution comprising 201 TD controls (i.e., one for each element). Hence, in this case the employment of the randomly-overlapped subarrays yields to a saving in the number of steering controls by approximately 68% off with respect to the conventional array design.

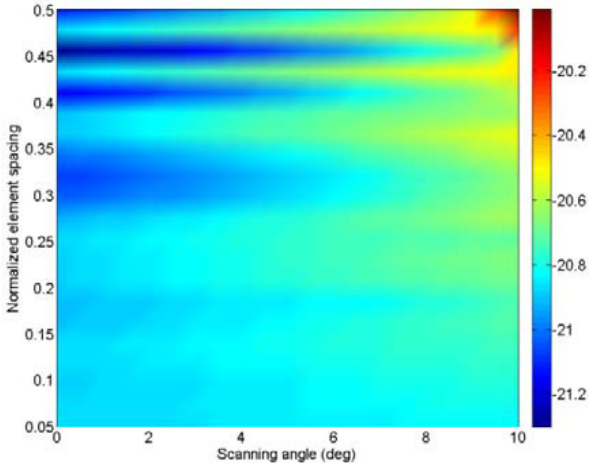

Figure 3. Peak sidelobe level as a function of the scanning angle and normalized inter-element spacing.

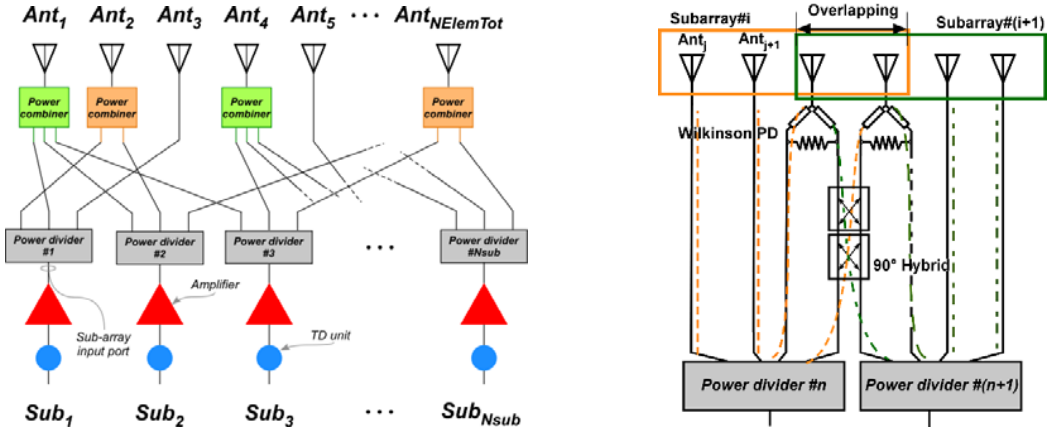

Figure 4. Proposed ROSA array: (a) example of the beamforming network and (b) microstrip-line implementation of a 2-element overlap belonging to two overlapped subarray.

An example of the beamforming network associated with the proposed ROSA array is reported in Fig. 4(a). It is important to underline that some of the *NElemTot* antennas are shared by one or more subarrays Sub_i $(i = 1, 2, \ldots, N_{sub})$, as also expressed in Fig. 4(a), thus requiring a different power combiner. Moreover, each subarray has its own fixed power divider, *Power divider#i* $(i = 1, 2, \ldots, N_{sub})$, which implements the proper power distribution for the overlap. The overall BFN always comprises a number of steering units and power divider equal to *Nsub*. The number of power combiners is determined by the level of overlapping. For example, if the case reported in Fig. 4(a) is considered, the BFN includes 116 two-way power combiners (number of elements belonging to two different subarrays) and 4 three-way power combiners (number of elements belonging to three different subarrays). From a hardware point of view, the physical implementation of the overlapped beamforming network depends on the operating frequency. Regarding the HF range, all the components can be simply connected through cables. At microwaves, the overlap can be realized in microstrip technology by commonly used printed circuit board processes. A possible schematic design to create overlap on a single-layer PCB is reported in Fig. 4(b) where two mid-radiating elements are shared across two adjacent 4-element subarrays. The crossover of the two innermost subarray output ports can be performed by cascading two quadrature hybrids. A Wilkinson power combiner can make the final signal combination at the element. The elements belonging to each one of the two overlapped subarrays are highlighted as well as the signals

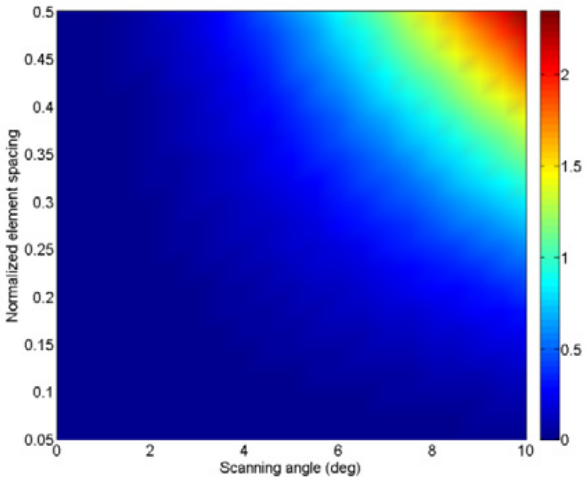

Figure 5. Proposed ROSA array: beamforming losses (dB) for the investigated array as a function of scanning angle and element spacing.

coming from the power dividers that feed each single antenna.

An evaluation of the BFN losses is illustrated in Fig. 5 as a function of the scanning angle and element distance. As it is apparent, the losses are less than 1 dB up to a scan angle of 6° for all frequencies and are more than 2 dB only around the maximum angular scan of 10°, being the input signals at the power combiners more and more out of phase as the scan increases.

4. PERFORMANCE ASSESSMENT OF RANDOMLY OVERLAPPED SUBARRAYS

To assess the performance of a ROSA configuration, a plurality of linear antenna array layouts, whose aperture size is approximately 100 wavelengths at the maximum operating frequency, has been investigated. Three different arrays exhibiting a maximum positive angular sweep of 5°, 7.5° and 10° were considered. The requirement on the array performance is to exhibit a peak SLL lower than −20 dB over all the considered angular sweeps. To this aim, we performed an exhaustive search in the space defined by the number of subarrays (*NSub*) and the number of elements per subarray (*NElemSub*). All the couples (*Nsub*, *NElemSub*) that determine a ROSA satisfying the constraint are collected in Fig. 5. It is apparent that a large number of solutions can be adopted by the designer, each one fulfilling the imposed requirement on the peak SLL although with a different number of subarrays (i.e.,

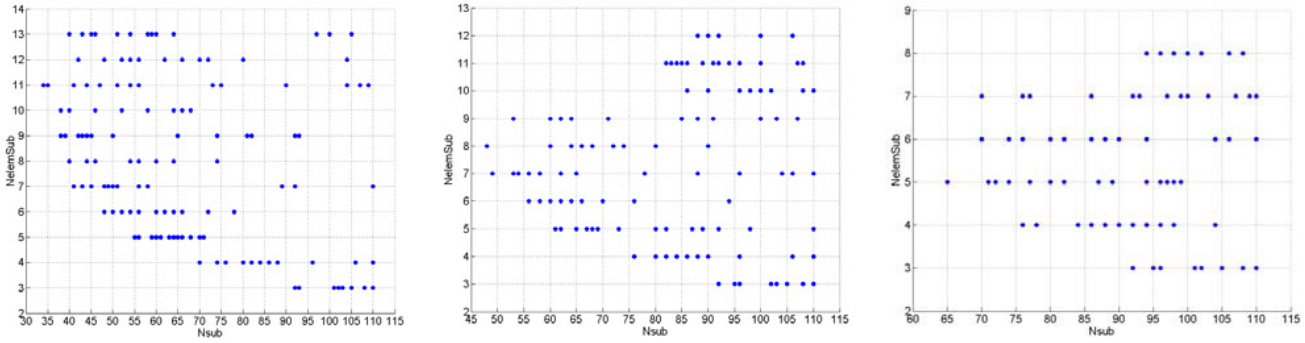

(a) (b) (c)

Figure 6. ROSA array configurations able to satisfy the requirement of a peak SLL lower than −20 dB for a linear extension of 100 wavelengths. The array design is provided in terms of *Nsub* and *NelemSub* in the case of a maximum scanning angle of: (a) 5°, (b) 7.5° and (c) 10°.

different degree of overlapping). For example, an array able to scan the main beam up to 5° from broadside direction with a peak SLL lower than the assigned threshold of −20 dB can be obtained with 40 subarrays ($NSub = 40$), each one comprising 13 elements ($NelemSub = 13$) or with 110 subarrays with 3 elements. In the former case the degree of overlap reaches 147% whereas in the latter is around 64%. Obviously, an array with a larger number of subarrays requires more TD units to scan the beam but a higher degree of overlap requires the employment of more power combiners with an increasing number of input ports. Therefore, the design can be cast also as a multi-objective problem [16] where the number of TD controls and power combiners of the ROSA can be considered the two target cost functions, under the constraint of a minimum acceptable peak SLL.

In order to estimate a lower bound on the number of components required by the proposed ROSA-BFN, three array aperture sizes, respectively equal to 50λ, 100λ, and 200λ, were investigated for three different maximum positive scanning angles, respectively of 5°, 7.5° and 10°. The constraint on the requested pSLL was kept fixed at a value of −20 dB for all the aforementioned cases. All the individuated

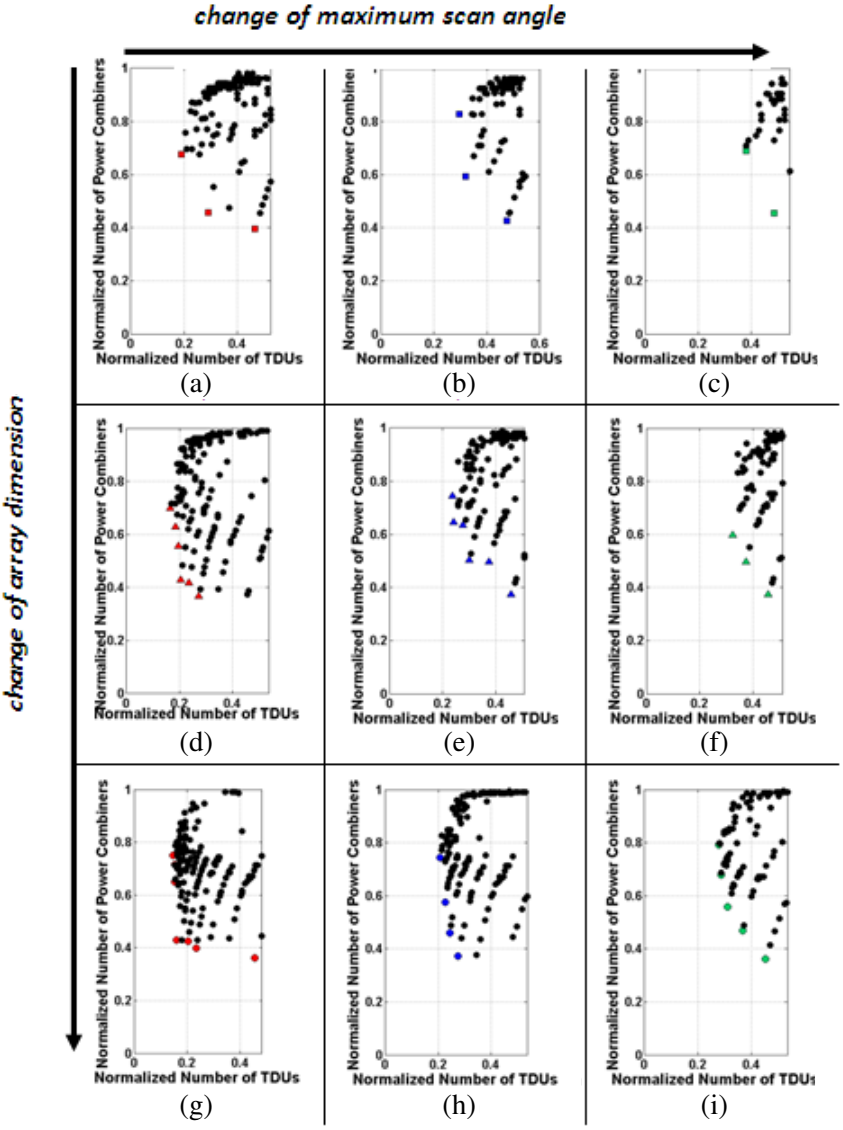

Figure 7. ROSA array configurations for different array size and various scan angles. In particular: (a)–(c) 50λ, (d)–(f) 100λ and (g)–(i) 200λ; (a), (d) and (g) refer to a scan angle of 5 deg, (b), (e) and (h) to 7.5 deg, (c), (f) and (i) to 10 deg.

solutions relative to each one of the nine combinations (array size, maximum scan angle) are reported in a separate subplot of Fig. 6. In particular, for a fair comparison among different-size arrays, each solution that satisfies the constraint on the pSLL is represented in a cartesian plot. The x-axis expresses the *Normalized Number of TDUs* (*NNTDU*), which is the ratio between the number of TD employed in that solution (*#TDUs*) and the overall number of elements (*NelemTot*). The y-axis represents the *Normalized Number of Power Combiners* (*NNPC*), which is the ratio between the number of combiners adopted in that configuration and the overall number of elements (*NelemTot*). All the identified solutions are represented in the cartesian plot but more emphasis is given to those solution that dominate in the Pareto sense [9, 16] which are highlighted by a different colored marker. Each one of these solutions represents a configuration that offers, at least, one cost function value that is not outperformed by any of the other configurations.

Next, by considering only the dominant solutions and applying again the Pareto dominance criterion, it is possible to summarize all the results as illustrated in Fig. 7. It is worthwhile to notice that the most important saving on the number of TD units and power combiners is achieved for large array, once the FOV half-maximum scan angle is fixed. However, for a fixed array dimension the *NNPC* spans approximately the same interval [0.35, 0.8] for any angle whereas the *NNTDU* is much more dependent on the maximum scan direction. For example, for an array dimension of 200λ the *NNPC* always spans the interval [0.35, 0.8] but the *NNTDU* is subject to a large variation since its value is around 0.15 for 5 deg but it is within [0.28, 0.46] for 10 deg. Once the array size is fixed, the larger is the beam scan the lower is the saving in the number of controls. On the other hand, once the desired angular scan is fixed, increasing the array size yields to a higher reduction of the number of controls up to more than 85% in the case of 5 deg and an array aperture of 200λ. Therefore, a larger scan angle forces to use a higher number of minimum controls. It is also interesting to check the complexity of the BFN that the investigated configurations require. For this purpose the kind of power combiners that has to be employed, has been investigated for all the aforementioned array layouts and it results that

Table 2. Radiation performance of the three ROSA arrays.

	Array aperture size		
	50λ	**100λ**	**200λ**
Total number of elements	103	201	403
Number of subarrays (*Nsub*)	39	65	112
Number of elements per subarray (*NElemSub*)	5	5	7
Maximum overlapping	3	3	3

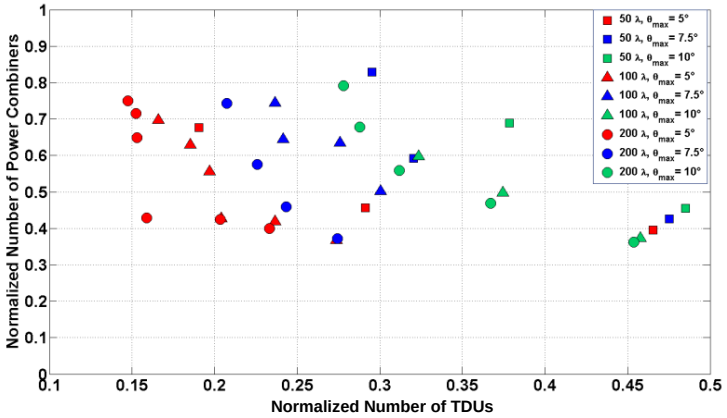

Figure 8. Final result of the merge of all the dominant solutions found for each couple (array size, scan angle).

the BFN of the ROSA requires a power combiner whose input ways never exceed 3 in all the cases.

With the aim of showing the effectiveness of the proposed beamforming technique, the radiating performance of the three array layouts, which possess the minimum number of controls as well as the largest scan herein considered, were selected for each investigated array aperture size. The main parameters of each array configuration are listed in the following Table 2, where the maximum overlapping is defined as the maximum number of overlapped subarrays that share the same radiating element across the array.

The geometries of the three different-sized linear arrays, respectively 50-λ, 100-λ and 200-λ long, are plotted in the corresponding Fig. 8(a), Fig. 8(b) and Fig. 8(c). An inter-element distance $d = \lambda/2$ has been selected in order to completely avoid the presence of grating lobes in the visible region of the subarray radiation pattern, as evident from Figs. 9(a), (c) and (e). The overall array pattern of Fig. 9(b), Fig. 9(d) and Fig. 9(f) has been evaluated by neglecting the contribution of any element factor. The benefits of aperiodically placing the subarray phase centers arise from Figs. 9(a), (c) and (e), where

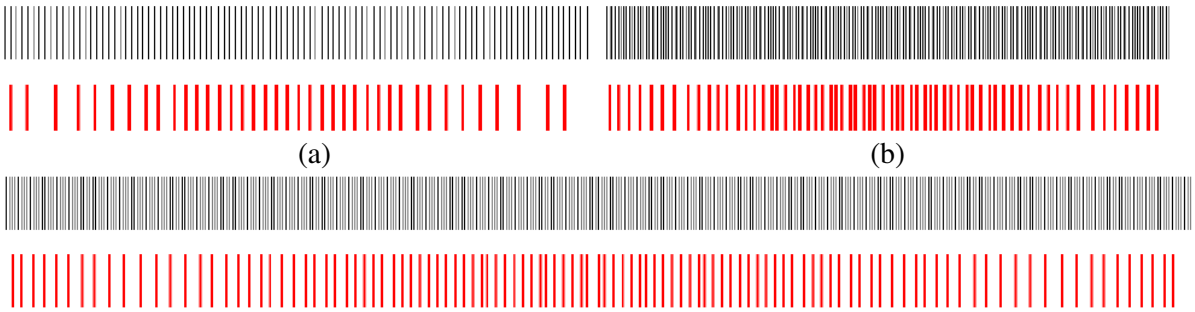

Figure 9. Array layout with the location of each element (black line) and the place of the subarray sources (red lines) for the three investigated arrays of length (a) 50λ, (b) 100λ and (c) 200λ.

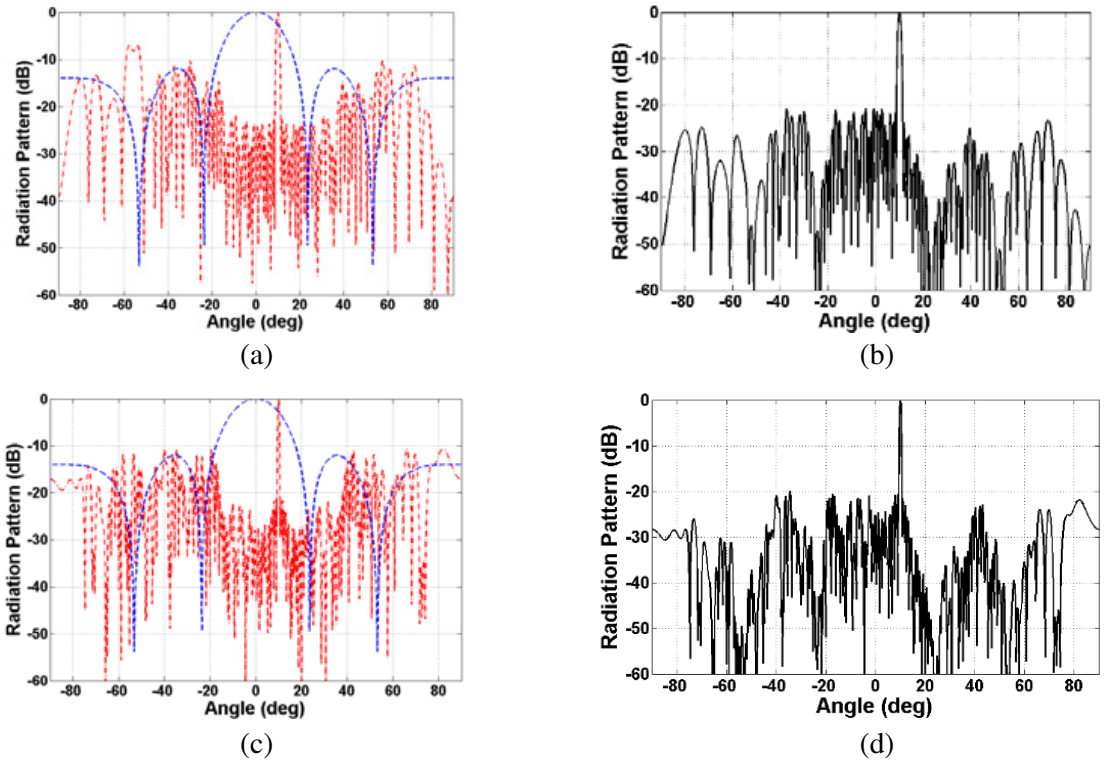

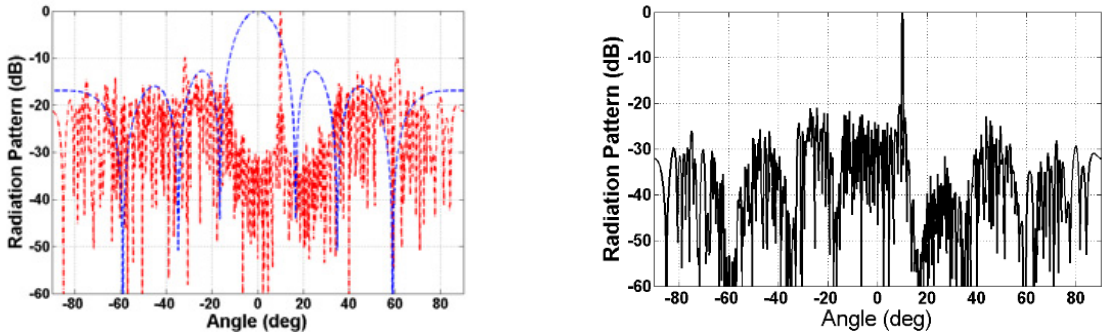

Figure 10. Superposition of the subarray radiation pattern (blue dashed line), array factor (red dashed line) and overall ROSAs array pattern (black line). Plot (a) and (b) refers to the 50λ array size, (c) and (d) to the 100λ one whereas (e) and (f) to the 200λ array.

the array factor sidelobe level is kept to a low level in the passband of the subarray pattern. This strategy allows achieving a low pSLL of the total array pattern while the main beam is scanned within the given scanning angle. In addition, by mean of the proposed overlapped subarray technique, the number of controls is reduced in comparison with the conventional arrays design, where both weighting and steering units have to be applied at element level.

5. CONCLUSIONS

This paper investigate the array architecture based on the randomly-overlapped subarrays (ROSAs) paradigm for the design of angular-limited scan systems. In the ROSAs array, antennas are shared by one or more subarrays that are randomly-overlapped. The comparison with a contiguous subarray arrangement and uniformly-overlapped scheme has provided a benchmark for highlighting the benefits offered by the proposed array configuration. The randomness of the subarray arrangement reduces the pSLL and prevents the rise of grating lobes in the scanning region. Different array sizes and scan directions have been considered, and the ROSAs array performance has been analyzed. As a result, it has been proved that the ROSAs beamforming network allows achieving a lower peak side lobe level, compared to the continuous and uniform overlapped schemes. Moreover, it has also been observed that even a moderate overlapping in ROSA provides a reduction of the number of controls with respect to the two aforementioned geometries. The comparison among three different array topologies (contiguous, uniform overlapped and randomly-overlapped subarrays) proves the superior performance of the ROSA approach in terms of peak sidelobe level in angular-limited scan arrays.

REFERENCES

1. Trinh-Van, S., H. B. Kim, G. Kwon, and K. C. Hwang, "Circularly polarized spidron fractal slot antenna arrays for broadband satellite communications in Ku-band," *Progress In Electromagnetics Research*, Vol. 137, 203–218, 2013.
2. Siakavara, K., "Novel fractal antenna arrays for satellite networks: Circular ring Sierpinski Carpet arrays optimized by genetic algorithms," *Progress In Electromagnetics Research*, Vol. 103, 115–138, 2010.
3. Rao, S. K., "Advanced antenna technologies for satellite communications payloads," *IEEE Transactions on Antennas and Propagation*, Vol. 63, No. 4, 1205–1217, Apr. 2015.
4. Massa, A., M. Donelli, F. G. B. D. Natale, S. Caorsi, and A. Lommi, "Planar antenna array control with genetic algorithms and adaptive array theory," *IEEE Transactions on Antennas and Propagation*, Vol. 52, No. 11, 2919–2924, Nov. 2004.

5. Mailloux, R. J., "A low-sidelobe partially overlapped constrained feed network for time-delayed subarrays," *IEEE Transactions on Antennas and Propagation*, Vol. 49, No. 2, 280–291, Feb. 2001.
6. Petrolati, D., P. Angeletti, and G. Toso, "A lossless beam-forming network for linear arrays based on overlapped sub-arrays," *IEEE Transactions on Antennas and Propagation*, Vol. 62, No. 4, 1769–1778, Apr. 2014.
7. Caille, G. and E. Girard, "Non-regular array solutions assessed from industrial point of view," *EuCAP 2014*, 3137–3141, 2014.
8. Spence, T. G., D. H. Werner, and J. N. Carvajal, "Modular broadband phased-arrays based on a nonuniform distribution of elements along the Peano-Gosper space-filling curve," *IEEE Transactions on Antennas and Propagation*, Vol. 58, No. 2, 600–604, Feb. 2010.
9. Bianchi, D., S. Genovesi, and A. Monorchio, "Constrained pareto optimization of wide band and steerable concentric ring arrays," *IEEE Transactions on Antennas and Propagation*, Vol. 60, No. 7, 3195–3204, Jul. 2012.
10. Morabito, A. F., T. Isernia, M. G. Labate, M. Durso, and O. M. Bucci, "Direct radiating arrays for satellite communications via aperiodic tilings," *Progress In Electromagnetics Research*, Vol. 93, 107–124, 2009.
11. Pierro, V., V. Galdi, G. Castaldi, I. M. Pinto, and L. B. Felsen, "Radiation properties of planar antenna arrays based on certain categories of aperiodic tilings," *IEEE Transactions on Antennas and Propagation*, Vol. 53, No. 2, 635–644, Feb. 2005.
12. Poli, L., P. Rocca, M. Salucci, and A. Massa, "Reconfigurable thinning for the adaptive control of linear arrays," *IEEE Transactions on Antennas and Propagation*, Vol. 61, No. 10, 5068–5077, Ottobre, 2013.
13. Haupt, R. L., "Thinned arrays using genetic algorithms," *IEEE Transactions on Antennas and Propagation*, Vol. 42, No. 7, 993–999, Jul. 1994.
14. Mailloux, R. J., S. G. Santarelli, T. M. Roberts, and D. Luu, "Irregular Polyomino-shaped subarrays for space-based active arrays," *International Journal of Antennas and Propagation*, Vol. 2009, 1–9, 2009.
15. Munk, B., *Finite Antenna Arrays and FSS*, Wiley, 2003.
16. Coello, C. C., G. B. Lamont, and D. A. van Veldhuizen, *Evolutionary Algorithms for Solving Multi-objective Problems*, Springer Science & Business Media, 2007.